NUMERICAL COMPUTATION
OF DYNAMIC STRESS INTENSITY FACTORS
BY A LAGRANGIAN FINITE-DIFFERENCE METHOD
(THE HEMP CODE)

Y. M. Chen

April 2, 1974

LAWRENCE
LIVERMORE
LABORATORY
University of California/Livermore

LAWRENCE LIVERMORE LABORATORY
University of California / Livermore, California 94550

UCRL-51563

NUMERICAL COMPUTATION
OF DYNAMIC STRESS INTENSITY FACTORS
BY A LAGRANGIAN FINITE-DIFFERENCE METHOD
(THE HEMP CODE)

Y. M. Chen[*]

MS. date: April 2, 1974

[*]Permanent address: Department of Applied Mathematics and Statistics
State University of New York at Stony Brook
Stony Brook, N. Y. 11790

NUMERICAL COMPUTATION
OF DYNAMIC STRESS INTENSITY FACTORS
BY A LAGRANGIAN FINITE-DIFFERENCE METHOD
(THE HEMP CODE)

Abstract

Numerical computation of the dynamic stress intensity factor for a centrally cracked rectangular bar, subjected to uniaxial tensions in plane strain geometry with Heaviside-function time dependence, is carried out using the time-dependent Lagrangian finite-difference code, HEMP. Excellent agreement is found with results obtained from other methods. This demonstrates the capability and the reliability of the HEMP code as an extremely useful numerical method for solving dynamic problems in fracture mechanics. Also discussed is the dynamic behavior of the stress intensity factor and crack opening.

Introduction

The knowledge of the stress field in the vicinity of a crack is a prerequisite to the prediction of fracture and failure of the material. In order for the crack to propagate, the stress at the crack tip must exceed some critical value. For brittle materials, the linear elasticity model usually gives a reasonably good description of the macroscopic phenomena of fracture in solids. However, for this model it is well known that regardless of the magnitude of the applied load the stress at the tip of a crack may have a singularity of $O(r^{-1/2})$, where r is the radial distance from the crack tip to the point of observation.[1-4] To overcome the analysis difficulty that an infinite stress assumption causes, the stresses in the neighborhood of the crack tip are normalized by multiplying them by a function $O(r^{1/2})$, yielding zero at the crack tip. This leads to the definition of the stress intensity factors.[3] For dynamic problems, the dynamic stress intensity factor is defined in the same manner as for the static case. The only difference is that the dynamic stress intensity factor is a function of time t.

Recently, considerable research has been done on the determination of the dynamic stress fields around a finite crack in an infinite elastic solid.[5-15] However, the quasi-numerical methods used are incapable of solving dynamic problems with finite boundaries. On the other hand, the finite element method can be used to solve problems in fracture mechanics with finite boundaries provided

-1-

the loads are static.[16-20] Actually,
finite element methods can be used for
dynamic problems by applying a series of
incremental static loads to approximate
time variations.[21-23] This approach re-
quires inordinate amounts of computer
time for two- and three-dimensional prob-
lems when a large number of elements
are used, because a large set of simulta-
neous linear algebraic equations must be
solved at each time step. It becomes
especially inefficient when large matrices
occur as in calculations involving three
space dimensions. The work presented
here is concerned with the solution of
problems involving dynamic fracture with
finite boundaries using finite difference
methods, which avoid the difficulties of
the finite element method.

The main mathematica' tool used is a
Lagrangian finite-difference computer
program, the HEMP code. The general
program can be used to solve problems
in three space dimension and time.[24-26]
In this paper we demonstrate the capabil-
ity and the reliability of the HEMP code
for solving dynamic problems in fracture
mechanics by applying it to a simple two-
dimensional but nontrivial dynamic problem.

For simplicity, a centrally cracked rec-
tangular bar in plane strain geometry is con-
sidered. A uniaxial tension with a Heaviside-
function time dependence is applied. The
details of the example are given in the next
section, and the numerical results are
presented graphically in the third section.
Finally, in the last section, a detailed dis-
cussion of the numerical results is given

Example Problem

Consider a rectangular bar with a cen-
trally located crack shown in Fig. 1. It
is loaded dynamically in the axial direc-

tion by a uniform tension P(t) with
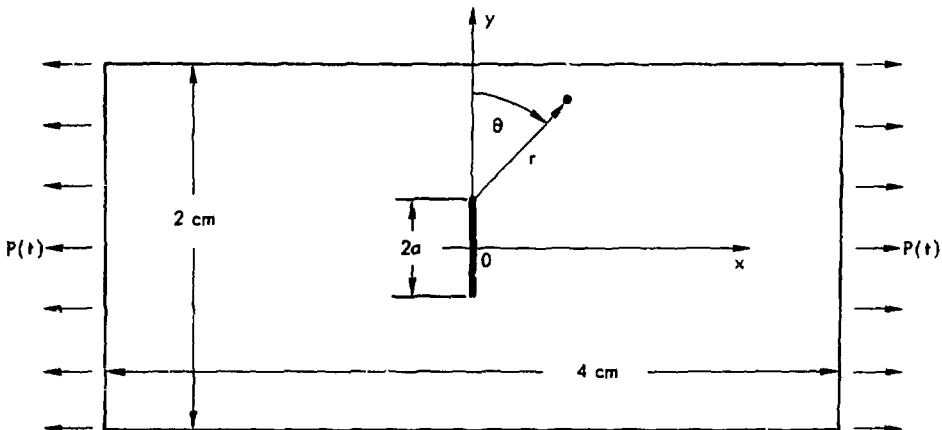Heaviside-function time dependence
(Fig. 2). The boundary conditions given

Fig. 1. Geometry of the bar in the example problem; a = 0.24 cm.
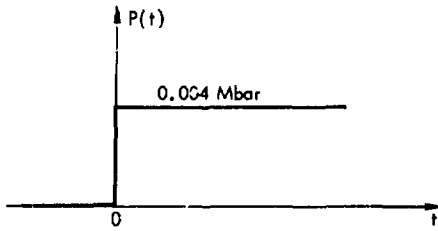
-2-

Fig. 2. Load curve assumed in example problem.

Fig. 3. Zoning of the quarter of the bar treated in the calculation.

correspond to plane strain loading. The bar is assumed to be a linear elastic material with the following characteristics:

Shear modulus $G = 0.76923$ Mbar,
Bulk modulus $K = 1.66667$ Mbar,
Poisson's ratio $\nu = 0.3$,
Density $\rho = 5$ g/cm^3.

Hence the longitudinal wave speed is

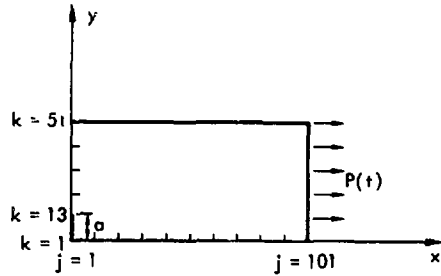$$v_L = \sqrt{\frac{K + \frac{4}{3} G}{\rho}} \approx 0.734 \text{ cm/}\mu\text{sec}, \qquad (1)$$

the transverse wave speed is

$$v_T = \sqrt{\frac{G}{\rho}} \approx 0.392 \text{ cm/}\mu\text{sec}, \qquad (2)$$

and the Rayleigh wave speed[27] is

$$v_R \approx 0.495 \, v_L \approx 0.363 \text{ cm/}\mu\text{sec}. \qquad (3)$$

By symmetry it is sufficient to solve the quarter problem, as shown in Fig. 3. A grid of 50 zones/cm was used.

Numerical Results

Due to the inability of any finite-difference method to represent the extremely steep stress gradients that occur in the neighborhood of a crack tip, a subroutine for extrapolation of the mode I dynamic stress intensity factor $k_1(t)$ from the stress field in the vicinity of the crack tip is used here. The procedure uses the stress field equations in the neighborhood of the crack tip ($r = 0$), assuming an infinite elastic medium,

$$\sigma_{im}(t) \approx \frac{k_1(t)}{(2\pi r)^{1/2}} f_{im}(\theta), \qquad (4)$$

where

$$f_{xx}(\theta) = \left(1 + \sin \frac{\theta}{2} \sin \frac{3\theta}{2}\right) \cos \frac{\theta}{2},$$

$$f_{yy}(\theta) = \left(1 - \sin \frac{\theta}{2} \sin \frac{3\theta}{2}\right) \cos \frac{\theta}{2},$$

$$f_{xy}(\theta) = f_{yx}(\theta) = \sin \frac{\theta}{2} \cos \frac{\theta}{2} \cos \frac{3\theta}{2}.$$

From (4) we define for every time step

$$k_1^*(n\Delta t) \equiv \frac{(2\pi r_{jk})^{1/2}}{f_{im}(\theta_{jk})} \sigma_{im}(n\Delta t). \qquad (5)$$

-3-
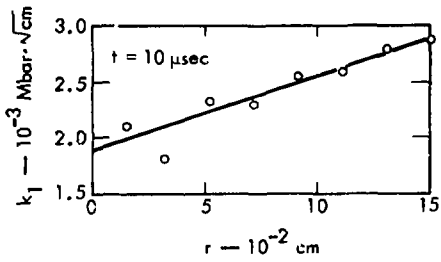
Here (r_{jk}, θ_{jk}) are the radial coordinates of a point (j,k) referred to the crack tip. Once the extrapolation path is chosen, Eq. (5) can be considered as a discrete functional relation between $k_1^*(n\Delta t)$ and

Fig. 4. A typical linear extrapolation curve for k_i.

Fig. 5. Curve of $\tilde{k}_1(t)$ vs t.

-4-

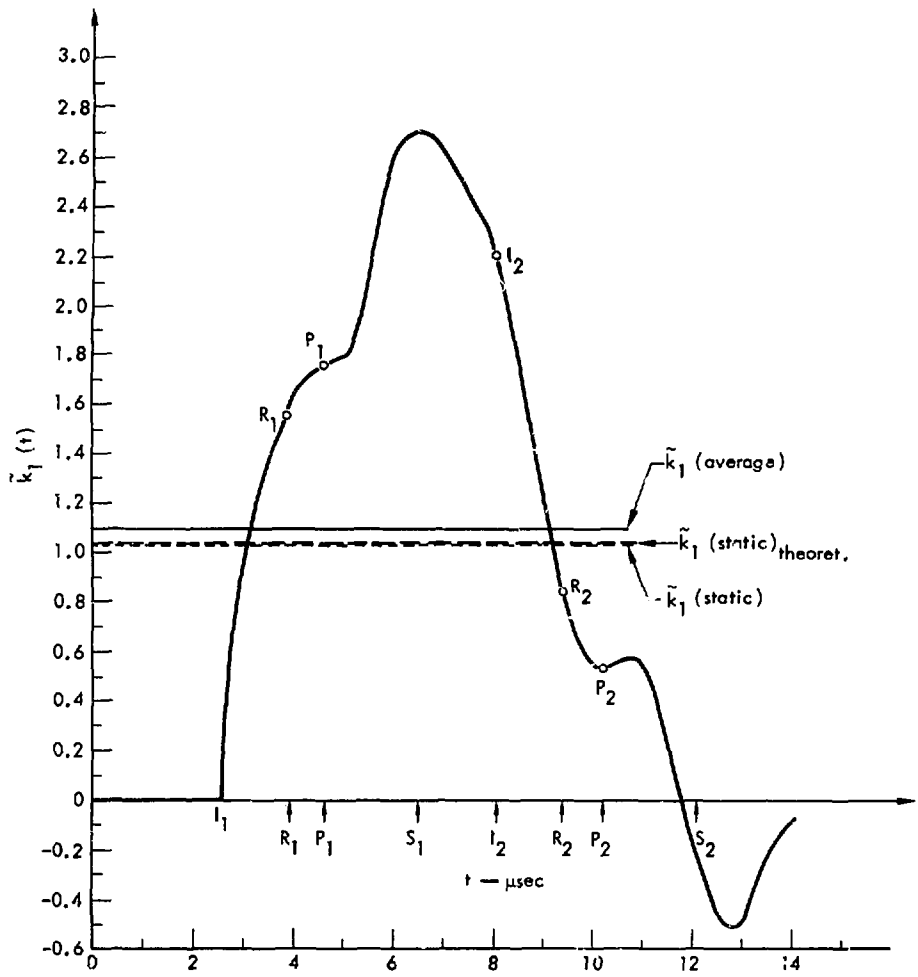r_{jk}. Our particular extrapolation path along the straight line $x = 0.01$ cm is the closest to the best path (see Appendix). Next, these discrete data are fitted by least-squares to a straight line,

$$k_1^*(n\Delta t) = k_1(n\Delta t) + \beta(n\Delta t)r, \qquad (6)$$

where $k_1(n\Delta t)$ is the approximate value of the mode I dynamic stress intensity factor at time $n\Delta t$. The error for this kind of straight-line extrapolation is $O(r^2)$ (see Appendix). Note that the data for two to three zones nearest to the crack tip are discarded in the least-squares curve fitting. Extrapolations along lines in several directions were also made.
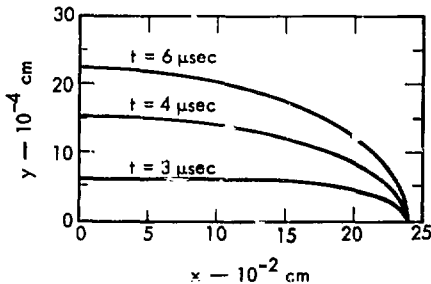
The final values agreed to within 5%. A typical plot of (5) and (6) is shown in Fig. 4. The normalized mode I dynamic stress intensity factor $\tilde{k}_1(t) = k_1(t)/P(t)(\pi a)^{1/2}$ is plotted against t in Fig. 5. Also, the geometry of the crack opening for several time steps is shown in Fig. 6. A σ_{xx} contour plot is given in Fig. 7. The above subroutine has been used successfully by others.[17,28]

Fig. 6. Geometry of the crack opening at three different time steps.

t = 3.57 μsec

Units are 100 MPa
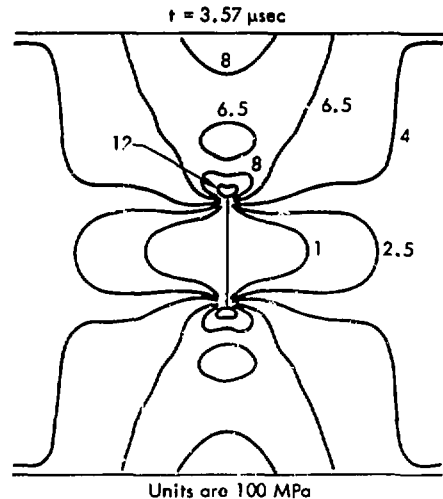
Fig. 7. A typical σ_{xx} contour (retraced from computer plot).

Discussion

If there were no crack in the rectangular bar, the stress field in the bar due to the dynamic loading P(t) of Fig. 2 would be a standing wave centered around the appropriate static value. However, in the presence of the crack there are many oscillations in the $\tilde{k}_1(t)$-vs-t curve. These oscillations are due to scattering

phenomena from the crack tip and the boundary surfaces.

On the time axis of Fig. 5, I_1 denotes the numerically computed (HEMP code) time needed for the incident longitudinal wave to travel to the crack from the bar ends. Now, the following times are computed from the wave velocities, Eqs. (1),

-5-

(2), and (3), and the true geometric distances: $(R_1 - I_1)$ denotes the time needed for the Rayleigh wave, generated by the initial incident waves, to travel between the two crack tips; $(P_1 - I_1)$ denotes the time needed for the scattered longitudinal wave, generated by the initial incident waves, to travel from a crack tip to the nearest boundary surface of the bar and back to the same tip; similarly, $(S_1 - I_1)$ corresponds to the scattered transverse wave; I_2 denotes the time needed for the incident longitudinal waves to travel the length of the bar, reflect from the boundary surface on the opposite side, and then travel back to the crack; analogous definitions are given to $(R_2 - I_2)$, $(P_2 - I_2)$, and $(S_2 - I_2)$ respectively, generated by these secondly incident longitudinal waves. Hence, with the help of these time marks one can identify the oscillations in the $\tilde{k}_1(t)$-vs-t curve as being caused by the cancellation and the reinforcement of the incident waves by various scattered waves. The σ_{xx}-vs-t curve (Fig. 8) at
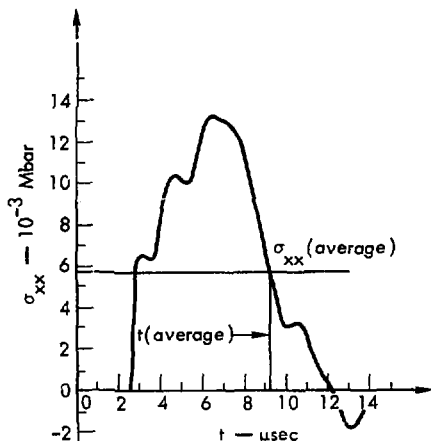

Fig. 8. The σ_{xx}-vs-t curve at (x, y) = (0.01 cm, 0.37 cm).

(x, y) = (0.01 cm, 0.37 cm) has the same general behavior as the $\tilde{k}_1$-vs-t curve except for the extra peak at $t \approx 3$ μsec due to the scattered longitudinal wave traveling directly from the nearest crack tip to the point (0.01 cm, 0.37 cm).

The normalized static stress intensity factor for the same problem but with static load of 4×10^{-3} Mbar at both ends of the bar can be estimated with reasonable accuracy, if the maxima and minima of $\tilde{k}_1(t)$ are not significantly altered by the dynamic oscillations. We believe that this is the case for our example. The simplest way to obtain $\tilde{k}_1$(static) is

$$\tilde{k}_1(\text{static}) = \frac{1}{2}[\text{Max } \tilde{k}_1(t) - \text{Min } \tilde{k}_1(t)]$$

$$- [\text{Min } \tilde{k}_1(t)] \, H(-\text{Min } \tilde{k}_1(t)) ,$$

where H is the unit Heaviside function, and Max f(t) and Min f(t) are the first global maximum and the first global minimum of f(t) respectively. Hence from Fig. 5 and the above formula, $\tilde{k}_1$(static) = 1.095, which is about 5.5% larger than the more accurate theoretical solution,[29] $\tilde{k}_1$(static) = 1.038. Since the dynamic $\tilde{k}_1$ has already incorporated an extrapolation, a more accurate method to obtain the static $\tilde{k}_1$ would be to use the calculated $\sigma_{xx}(t)$ a few zones away from the tip. Thus we obtain k_1(static) as follows: First obtain σ_{xx}(static) from Fig. 8.

$$\sigma_{xx}(\text{static}) = \frac{1}{2}[\text{Max } \sigma_{xx}(t) - \text{Min } \sigma_{xx}(t)]$$

$$- [\text{Min } \sigma_{xx}(t)] \cdot H(-\text{Min } \sigma_{xx}(t))$$

$$= 5.70 \times 10^{-3} \text{ Mbar.}$$

This stress value corresponds to t_s = 9.22 μsec. It is seen in Fig. 5 that for

$t = t_s$, $\tilde{k}_1$(static) = 1.028, which is about 1% less than the value given in Ref. 29. Thus we see that both the dynamic and static values of the stress intensity factor can be calculated with the time-dependent HEMP code.

It is important to notice that the dynamic stress intensity factors for a finite crack in an infinite elastic solid are found to be 15-30% greater than the analogous static value.[13,15] These phenomena are attributed to the scattered Rayleigh waves. If there were only one incident plane wave in our example, then due to the superposition principle in linear elasticity theory,

$$[\text{Max } \tilde{k}_1(t)]_{\text{one wave}}$$

$$= \frac{1}{2}[\text{Max } \tilde{k}_1(t)]_{\text{two waves}} = 1.35,$$

which is about 30% larger than the analogous static value. But for the two-wave case, the overshooting is about 160%. This shows that in a practical situation the overshooting of the dynamic stress intensity factor is attributed mainly to
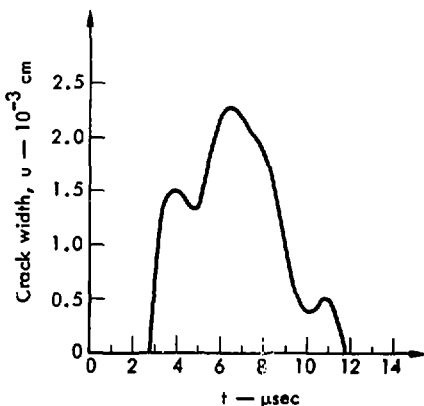
Fig. 9. The u-vs-t curve at the middle of the crack surface.

the particular geometry and the manner of loading.

The geometry of the crack opening and the opening and the closing of crack surfaces as functions of t are the natural products of the HEMP code calculation. They are plotted in Figs. 6 and 9, respectively. In general, the crack opens or closes when the crack tip experiences tension or compression, respectively.

Acknowledgments

Appendix
Error Analysis

In the neighborhood of the crack tip, assuming an infinite elastic medium,

$$\sigma_{xx}(r, \theta) = k_1 f_{-1/2}(\theta) r^{-1/2} + f_0(\theta) + f_{1/2}(\theta) r^{1/2} + f_1(\theta) r$$

$$+ f_{3/2}(\theta) r^{3/2} + f_2(\theta) r^2 + O(r^{5/2}), \tag{A-1}$$

where

$$f_{-1/2}(\theta) \neq 0, \text{ for } 0 \leq |\theta| < \pi.$$

It is well known[30] that the angular functions $f_n(\theta)$, $n = 0, 1, 2, \ldots$, have the special property

$$f_n(0) = 0, \quad n = 0, 1, 2, \ldots. \tag{A-2}$$

If we define

$$k_1^*(r, \theta) = \frac{r^{1/2}}{f_{-1/2}(\theta)} \sigma_{xx}(r, \theta), \tag{A-3}$$

then (A-1) and (A-2) yield

$$k_1^*(r, \theta) = k_1 + [f_{-1/2}(\theta)]^{-1} \left[f_0(\theta) r^{1/2} + f_{1/2}(\theta) r + f_1(\theta) r^{3/2} \right.$$

$$\left. + f_{3/2}(\theta) r^2 + f_2(\theta) r^{5/2} + O(r^3) \right]. \tag{A-4}$$

It is obvious that the best way to obtain higher accuracy is to choose the extrapolation path so that most of the f's vanish. In this particular case, the extrapolation path is along $\theta = 0$. From (A-2) and (A-4),

$$k_1^*(r, 0) = k_1 + [f_{-1/2}(0)]^{-1} \left[f_{1/2}(0) r + f_{3/2}(0) r^2 + O(r^3) \right]. \tag{A-5}$$

Hence a straight-line fit of $k_1^*(r, 0)$ will have an error $O(r^2)$, and a quadratic fit of $k_1^*(r, 0)$ will have an error $O(r^3)$.

References

1. H. M. Westergaard, "Bearing Pressures and Cracks," J. Appl. Mech., Trans. ASME 61, A-49 (1939).

2. I. N. Sneddon, "The Distribution of Stress in the Neighborhood of a Crack in an Elastic Solid," Proc. Phys. Soc. London 189, 229 (1946).

3. G. R. Irwin, "Analysis of Stresses and Strains Near the End of a Crack Traversing a Plate," J. Appl. Mech., Trans. ASME 24, 361 (1957).

4. M. L. Williams, "On the Stress Distribution at the Base of a Stationary Crack," J. Appl. Mech., Trans. ASME 24, 109 (1957).

5. B. V. Kostrov, "Motion of a Rigid Strip-Mass Soldered into an Elastic Medium, Excited by a Plane Wave," J. Appl. Math. Mech. 28, 113 (1964).

6. J. F. Loeber and G. C. Sih, "Diffraction of Antiplane Shear Waves by a Finite Crack," J. Acoust. Soc. Amer. 44, 90 (1968).

7. G. C. Sih and J. F. Loeber, "Wave Propagation in an Elastic Solid with a Line of Discontinuity or Finite Crack," Quart. Appl. Math. 27, 193 (1969).

8. J. D. Eshelby, "The Elastic Field of a Crack Extending Nonuniformly Under General Anti-Plane Loading," J. Mech. Phys. Solids 17, 177 (1969).

9. J. D. Achenbach "Crack Propagation Generated by a Horizontally Polarized Shear Wave," J. Mech. Phys. Solids 18, 245 (1970).

10. J. D. Achenbach, "Brittle and Ductile Extension of a Finite Crack by a Horizontally Polarized Shear Wave," Int. J. Eng. Sci. 8, 947 (1970).

11. A. K. Mal, "Interaction of Elastic Waves with a Penny-Shaped Crack," Int. J. Eng. Sci. 8, 381 (1970).

12. A. K. Mal, "Interaction of Elastic Waves with a Griffith Crack," Int. J. Eng. Sci. 8, 763 (1970).

13. S. A. Thau and T. H. Lu, "Transient Stress Intensity Factors for a Finite Crack in an Elastic Solid Caused by a Dilatational Wave," Int. J. Solids Structures 7, 731 (1971).

14. G. T. Embley and G. C. Sih, "Response of a Penny Shaped Crack to Impact Waves," Proc. 12th Midwestern Mechanics Conference (1971).

15. G. C. Sih, G. T. Embley, and R. S. Ravera, "Impact Response of a Finite Crack in Plane Extension," Int. J. Solids Structures 8, 977 (1972).

16. A. S. Kobayashi, D. E. Maiden, B. J. Simon, and S. Iida, "Application of Finite Element Analysis Method to Two-Dimensional Problems in Fracture Mechanics," ASME Paper No. 69-WA/PVP-12 (1969).

17. S. K. Chan, I. S. Tuba, and W. K. Wilson, "On the Finite Element Method in Linear Fracture Mechanics," Eng. Fracture Mech. 2, 1 (1970).

18. P. V. Marcal, "Three-Dimensional Finite Element Analysis for Fracture Mechanics," The Surface Crack: Physical Problems and Computational Solutions, Ed. by J. L. Swedlow (ASME, New York, 1972), papers presented at the Winter Annual Meeting of ASME.

19. P. D. Hilton and G. C. Sih, "Application of the Finite Element Method to the Calculation of Stress Intensity Factors," Mechanics of Fracture I: Methods of Analysis and Solutions of Crack Problems, Ed. by G. C. Sih (Noordhoff Int. Pub., Leyden, The Netherlands, 1973), p. 426.

20. W. K. Wilson, "Finite Element Methods for Elastic Bodies Containing Cracks," Mechanics of Fracture I: Methods of Analysis and Solutions of Crack Problems, Ed. by G. C. Sih (Noordhoff Int. Pub., Leyden, The Netherlands, 1973), p. 484.

21. E. H. Wu and E. A. Witmer, "Finite Element Analysis of Large Elastic-Plastic Transient Deformations of Simple Structures," AIAA J. 9, 1719 (1971).

22. J. F. McNamara and P. V. Marcal, "Incremental Stiffness Method for Finite Element Analysis of the Nonlinear Dynamic Problem," Proc. Int. Symp. Numerical and Computer Methods in Struct. Mech., Urbana, Ill., 1971.

23. M. Hartzman and J. R. Hutchinson, "Nonlinear Dynamics of Solids by the Finite Element Methods," Comp. Struct. 2, 47 (1972).

24. Mark L. Wilkins, "Calculation of Elastic-Plastic Flow," Methods in Computational Physics, Ed. by B. Alder, S. Fernbach, and M. Rotenberg (Adademic Press, New York and London, 1964), Vol. 3, p. 211-262.

25. Mark L. Wilkins, Calculation of Elastic-Plastic Flow, Lawrence Livermore Laboratory, Rept. UCRL-7322 Rev. 1 (1969); or International Coll. on Gasdynamics of Explosions – Reactive Systems, Moscow, USSR (1969), p. 408.

26. Mark L. Wilkins, S. J. French, and M. Sorem, "Finite Difference Scheme for Calculating Problems in Three Space Dimensions and Time," Proceedings of the Second International Conference on Numerical Methods in Fluid Dynamics, Ed. by M. Holt, Lecture Notes in Physics Series (Springer-Verlag, New York, 1971), Vol. 8, pp. 30-33.

27. Y. C. Fung, Foundations of Solid Mechanics (Prentice-Hall, Englewood Cliffs, N. J., 1965).

28. T. A. Cruse, "Numerical Evaluation of Elastic Stress Intensity Factors by the Boundary-Integral Equation Method," The Surface Crack: Physical Problems and Computations, Ed. by J. L. Swedlow (ASME, New York, 1972), papers presented at the Winter Annual Meeting of ASME.

29. A. S. Kobayashi, R. D. Cherepy, and W. C. Kinsel, "A Numerical Procedure for Estimating the Stress Intensity Factor of a Crack in a Finite Plate, J. Basic Eng. Trans. ASME, Ser. D. 86, 681 (1964).

30. J. P. Benthem and W. T. Koiter, "Asymptotic Approximations of Crack Problems," Mechanics of Fracture I: Methods of Analysis and Solutions of Crack Problems, Ed. by G. C. Sih (Noordhoff Int. Publ., Leyden, The Netherlands, 1973), p. 131.